A Compact Cognitive Radio UWB/Reconfigurable Antenna System with Controllable Communicating antenna Bandwidth

Abdulghafor Abdulghafar Abdulhameed, Falih Mahdi Alnahwi, , Husham Lateef Swadi, Abdulkareem Swadi Abdullah

Abstract

A low profile and compact size cognitive radio (CR) sensing/communicating antenna system is presented in this paper. A slotted elliptical monopole antenna (SEMA) is proposed as an ultra-wideband (UWB) sensing antenna for the CR system, while the CR communication relies on a triangular reconfigurable monopole antenna. Two PIN diodes are attached to the reconfigurable antenna to provide four different wideband CR communications with variable bandwidths. The simulation and measured results are in good congruence, and they demonstrate that both antennas have an omnidirectional radiation pattern with acceptable gain values that are compatible with the portable CR gadgets. The variable wideband CR communication is also highlighted by the acquired measurements. In addition, the results show low mutual coupling between the sensing antenna and the communicating antenna that reaches to values less than -16dB for all operation modes of the PIN diodes.

Keyword

Reconfigurable antenna, Ultra-wideband, Mutual coupling, PIN-diode

1. Introduction

Recently, the researchers' interest of providing an efficient utilization for the wireless spectrum has increased noticeably due to the consumers demand for high data rate and high quality of communication. A new technology called cognitive radio (CR) has emerged to compensate the shortcomings of the original frequency spectrum allocation. This technology consists of a sensing system that searches for the presence of some idle frequency bands (white spaces) and another system to communicate through the detected bands [1]. The CR sensing part front end is attached to an ultra-wideband antenna (UWB) that scans the entire band specified for UWB applications (3.1-10.6GHz), whereas the front end of the communication part is connected to a frequency reconfigurable antenna to switch the communication frequency band to the idle bands [2]. The frequency reconfiguration of the communicating antenna can be accomplished with the aid of PIN diodes, varactor diodes, or any other radio frequency (RF) switches [3].

Generally, CR systems can be classified into two categories: the first is called underlay CR systems, and the other is known as interweave CR systems. The underlay CR system uses a single UWB antenna with reconfigurable band notch to avoid the interference with some critical applications during their active mode [4-8]. However, the interweave CR system, which is the main scope of this paper, requires two separated antennas one for sensing and the other for communication [9]. Since the interweave CR system includes two antennas, the mutual coupling between these two antennas should be maintained as low as possible in order to isolate the operation of the sensing part and the communication part of the overall CR system [10]. Several methods were suggested for mutual coupling reduction to values less than -15dB such as modifying the placement and the orientation of the antennas [11], inserting neutralization lines [12], and using a defected ground plane [13]. Generally speaking, the sensing antenna of the interweave CR is a UWB antenna, while the CR communicating antenna is either a single reconfigurable narrow band antenna [14] or a reconfigurable antenna with multi-narrow bands for each switching mode [15-17].

In this paper, a compact sensing/communicating antenna system is proposed for interweave CR applications. The sensing antenna is a slotted elliptical monopole antenna (SEMA) whose bandwidth covers the entire frequency band specified for the UWB applications (3.1-10.6GHz). With the aid of two PIN diodes, the triangular wide band reconfigurable communicating antenna can switch its frequency band to four different locations with different bandwidth coverage. Therefore, the system can support four different data rates based on the selected bandwidth. The antenna measurements are well agreed with the simulation results, and both of them verify the perfect UWB coverage of the sensing antenna and the switchable wideband coverage of the communicating antenna in addition to the low mutual coupling between the two antennas. Moreover, the results reveal an omnidirectional pattern for both antennas suitable for portable interweave CR devices.

2. Antenna Structure and Parametric Study

Figure 1 illustrates the geometry and the overall dimensions of the front and the back views of the proposed antenna system. The antenna is engraved on Rogger 5880 dielectric substrate with height $\mathrm{h} = 0.8\mathrm{mm}$ and dielectric constant $\varepsilon_r = 2.23$. The overall dimensions of the proposed antenna system are $50 \times 30 \times 0.8\, mm^3$. The following two subsections study in detail the dimensions and parameters of the sensing antenna and the communicating antenna. The antenna system is simulated using the Computer Simulation Technology CST Microwave Studio software [18].

2.1 Communicating Antenna Design

As mentioned earlier, the communicating antenna is a reconfigurable triangular monopole antenna whose dimensions are illustrated in Figure 2. Two PIN diodes are used to control the antenna center frequency and bandwidth according to the operation mode of each of them. The PIN diodes used in this work are SMP1320-079LF with forward biasing resistance value of ($R_f = 0.9\Omega$ at $10mA$) and reverse biasing capacitor of ($C_r = 0.3pF$). The PIN diode ON state is simulated by placing resistance equal to the value of the forward biasing resistance, while the reverse biasing capacitor simulates the OFF state of the PIN diode.

Four different cases are obtained for each operation mode of the PIN diodes. The magnitude of the reflection coefficient of the communicating antenna $|S_{11}|$ corresponding to each PIN diode state is shown in Figure 3. When PIN diode-1 and PIN diode-2 are at their OFF state, the antenna bandwidth is 1.75GHz along the frequency range (4.25-6GHz), and the resonant frequency is located at 4.85GHz. The second mode happens when PIN diode-1 is OFF and diode-2 is ON. In this case, the antenna is operating as a dual wide band antenna, but the impedance matching holds only the second band which resonates at 6.7GHz with antenna bandwidth equal to 0.75GHz extended along the range (6.6-7.35GHz). The third case is achieved when PIN diode-1 is ON and PIN diode-2 is OFF. This operation mode provides impedance matching for both bands generated at case 2. Since the two bands are close to each other, they overlap to form single wide band centered at 5.7GHz with antenna bandwidth equal to 2.9GHz over frequency range of (4.25-7.15GHz). Finally, when both PIN diodes are ON, the impedance matching of this mode is centered at 5.2GHz with bandwidth of 1GHz along the frequency range (5-6GHz). It is clear that the antenna has noticeably variable bandwidth depending on the operation mode of the PIN diodes, so the antenna can support different data rates according to the available idle frequencies detected by the sensing antenna.

2.2 Sensing Antenna Design

The UWB band (3.1-10.6GHz) is scanned by using the slotted elliptically monopole antenna (SEMA) shown in Figure 4. L and W represent the length and width of the sensing antenna, respectively, and $g = 1mm$ is the gap between the ground plane and the elliptical patch. This patch is inspired from the circular monopole antenna CMA with some modifications. A 50Ω feeding matching line with $w_f = 2mm$ is fixed along the minor axis of the elliptical shape. The lower resonant frequency (f_l) of the elliptical antenna can be predicted from the following formula [19]:

$$f_l = \frac{72}{2a_1 + \frac{b_1}{4} + g} \text{ GHz} \tag{1}$$

where, $a_1$and b_1 are the major and minor axes of the patch, respectively. Figure 5 illustrates the magnitude of the reflection coefficients $|S_{22}|$ of the sensing antenna for different values of $a_1$and b_1.

The axial ration (a_1/b_1) modifies the location of the first resonant frequency of the monopole antenna because they modifies the electrical length of the antenna patch [19]. The values of $a_1$and b_1 are selected to be 11mm and 10mm, respectively, to set the lower frequency edge of the sensing antenna at 3GHz which is so close to the lower frequency edge of the UWB frequency band (3.1GHz).

The middle and higher frequency edge of the reflection coefficient can be controlled by the ground plane size of the sensing antenna. Figure 6 demonstrates the effect of the ground plane width on the reflection coefficient of the sensing antenna. It is clear that ground plane width of 24mm provides the widest antenna bandwidth compared to the other ground plane width values.

Lastly, a wide slot is etched at the upper edge of the sensing antenna to reduce the mutual coupling between the sensing and the communicating antennas without affecting the impedance matching of the sensing antenna. Figure 7 shows the magnitude of the transmission coefficient $|S_{21}|$ of the proposed antenna system for different slot length values. Slot length equal to 10mm produces a mutual coupling less than -16dB for the entire band of operation. To verify the minor effect of the slot on the sensing antenna impedance matching, Figure 8 is presented to compare the reflection coefficient of the sensing antenna with and without the slot, and it shows a negligible effect on the antenna bandwidth within the frequency range specified for the UWB applications. Table 1 concludes the sensing antenna parameters after the aforementioned modification process. To fortify the idea of the low mutual coupling between the two antennas, Figure 9 is presented to demonstrate the current distribution of the proposed antenna system at a frequency within the operating band of the communicating antenna when PIN diode-1 is ON and PIN diode-2 is OFF. It is obvious from this figure that the excitation of one antenna produces a negligible amount of current at the other antenna, and this verifies the large isolation between the two antennas.

Table 1: The parameters of the proposed UWB sensing antenna.

Parameter	L	W	Lg	Wg	Wf	g	a1	b1	Sl
Value (mm)	35	30	10.5	24	2	1	11	10	10

3. Fabrication and Measurement

The prototype of the proposed antenna system is shown in Figure 10. The fabrication and measurement process was held at Department of Electrical Engineering/University of Basrah using AMITEC network analyzer. As mentioned previously the PIN diode used in this design is SMP1320-

079LF with forward biasing resistance value ($R_f = 0.9\Omega$ at $10mA$) and reverse biasing capacitor of ($C_r = 0.3pF$). The blocking capacitor-1 ($30pF$) is inserted to the antenna in order to separate the biasing of each PIN diode, whereas blocking capacitor-2 is used to separate the positive biasing lines from the negative one. The deviation between the simulation and measurements is caused by many factors such as the fabrication imprecision, the imperfect soldering of the SMA connector and the PIN diodes, and the misalignment of the PIN diode and the blocking capacitor.

3.1 UWB Sensing Antenna Measurements

Figure 11 illustrates the simulated and measured reflection coefficients of the sensing antenna. The UWB coverage of each reflection coefficient can clearly be seen in this figure. The simulated and measured power patterns at the E-plane and H-plane of the sensing antenna at its resonant frequencies are shown in Figure 12. The pattern is bidirectional at the E-plane and almost omnidirectional at the H-plane which is suitable for portable cognitive radio sensing devices. The simulated and measured gain of the proposed sensing antenna as a function of frequency is illustrated in Figure 13. The antenna has reasonable gain values for the entire band assigned for UWB applications.

3.2 Reconfigurable Antenna Measurements

The simulated and measured reflection coefficients of the reconfigurable communicating antenna for different PIN diode states are shown in Figure 14, and the four different wide band coverage of the antenna is clearly notified in this figure. As discussed previously in Section 2, the communicating antenna has variable bandwidth for each PIN diode state which follows the availability of the idle bands in the wireless spectrum. This variable bandwidth qualifies the CR system to be operated at variable data rate which is directly proportional to the available bandwidth of the entire communication system. Table 2 summarizes the measured and simulated center frequency, bandwidth, and the gain of the proposed communicating antenna for different PIN diode states.

Table 2: The communicating antenna center frequency, bandwidth, and gain for different PIN diode states.

No.	PIN diode 1	PIN diode 2	Center Frequency (GHz)		Bandwidth (GHz)		Gain (dBi)	
			Simulated	Measured	Simulated	Measured	Simulated	Measured
1	off	off	4.85	4.73	1.75	1.45	1	0.92
2	off	on	6.7	6.9	0.75	0.83	0.75	0.64
3	on	off	5.7	5.62	2.9	2.8	2.574	2.334
4	on	on	5.4	5.3	1	0.93	2.5	2.32

The measured and simulated power patterns of the proposed communicating antenna are shown in Figure 15. Different diode states do not significantly influence the antenna power pattern, and this is one of the merits of the frequency reconfigurable antenna. In addition, the power pattern is almost omnidirectional for all PIN diode states, so the antenna is a good candidate for portable CR devices.

Finally, to highlight the mutual coupling between the sensing and the communicating antenna, Figure 16 shows the simulated and measured forward transmission coefficient $|S_{21}|$ of the antenna system. The antenna system has a reduced amount of coupling (less than -16dB) for the entire band of operation, and this verifies the good isolation between the two antennas.

5. Conclusion

A compact interweave CR antenna system with wide and variable communication bandwidth has successfully been designed and fabricated. The UWB sensing antenna perfectly covers the entire frequency band assigned for the UWB applications (3.-10.6GHz). The reconfigurable communicating antenna bandwidth and center frequency are controlled by the biasing state of two PIN diodes. Four different wide and variable antenna bandwidths are obtained to switch the operation of the CR system to four different communication data rates. The wide slot that is etched on the patch of the sensing antenna significantly reduces the mutual coupling between the sensing and the communicating antenna to values less than -16dB. The power patterns of both antennas are omnidirectional, which is compatible with the portable interweave CR devices.

References

[1] Y. Tawk, J. Costantine, and C. Christodoulou, Antenna Design for Cognitive Radio, Artech House, 2016.

[2] A.L.Hugine,“Antenna Selection for a Public Safety Cognitive Radio.”, M.Sc Disseration, Virginia Polytechnic Institute and State University, 2006

[3] CHRISTODOULOU, Christos G., et al. “Reconfigurable antennas for wireless and space applications”, Proceedings of the IEEE, 2012, Vol.100, no.7: 2250-2261.

[4] Mohammed, A. A., Alnahwi, F. M., Abdullah, A. S., & Hameed, A. G. A. A.” A compact monopole antenna with reconfigurable band notch for underlay cognitive radio applications. In: *Advance of Sustainable Engineering and its Application (ICASEA), 2018 International Conference on*. IEEE, 2018. p. 25-30

[5] G. Srivastava, S. Dwari, and B. K. Kanaujia, “A compact UWB antenna with reconfigurable dual notch bands,” Microwave and Optical Technology Letters, vol. 57, no. 12, pp. 2737–2742, 2015.

[6] H. A Atallah, A. B. Abdel-Rahman, K. Yoshitomi, and R. K. Pokharel, “Reconfigurable Band-Notched Slot Antenna Using Short Circuited Quarter Wavelength Microstrip Resonators,” Progress in Electromagnetics Research, vol. 68, pp. 119–127, 2016.

[7] H. Oraizi and N. V. Shahmirzadi, “Frequency-and time-domain analysis of a novel UWB reconfigurable microstrip slot antenna with switchable notched bands,” IET Microwaves, Antennas and Propagation, vol. 11, no. 8, pp. 1127–1132, 2017.

[8] F. Alnahwi and N. Islam, “A Generalized Concept for Band Notch Generation in Ultra-Wide Band Antennas,” Progress in Electromagnetic Research C, vol. 54, pp. 179-185, 2014.

[9] F. Alnahwi, A. Abdulhameed, and A. Abdullah, "A Compact Integrated UWB/Reconfigurable Microstrip Antenna for Interweave Cognitive Radio Applications," *International Journal on Communications Antenna and Propagation*, vol. 8, no. 1, pp. 81-86, 2018.

[10] HAMEED, A. G., et al. Mutual Coupling Reduction of a (2× 1) MIMO Antenna System Using Parasitic Element Structure for WLAN Applications. Department of Electrical Engineering, College of Engineering, University of Basrah, Basra, Iraq, 2015.
[11] K. L. Wong et al., "Isolation Between GSM/DCS and WLAN Antennas in a PDA Phone," Microwave and Optical Technology Letters, Vol. 45, No. 4, pp. 347–352, May 20, 2005.
[12] S. W. Su, C. T. Lee, and F. S. Chang, "Printed MIMO-Antenna System Using Neutralization-Line Technique for Wireless USB-Dongle Applications," IEEE Trans. On Antennas and Propagation, Vol. 60, No. 2, pp. 456–463, February 2012.
[13] J. F. Li, Q. X. Chu, and T. G. Huang, "A Compact Wideband MIMO Antenna with Two Novel Bent Slits," IEEE Trans. on Antennas and Propagation, Vol. 60, No. 2, pp. 482–489, February 2012.
[14] TAWK, Y.; CHRISTODOULOU, C. G. A new reconfigurable antenna design for cognitive radio. *IEEE Antennas and wireless propagation letters*, 2009, 8: 1378-1381.
[15] TARBOUSH, HF Abu, et al. Reconfigurable wideband patch antenna for cognitive radio. In: *Antennas & Propagation Conference, 2009. LAPC 2009. Loughborough*. IEEE, 2009. p. 141-144.
[16] SHARMA, Sonia; TRIPATHI, Chandra Charu. A wide spectrum sensing and frequency reconfigurable antenna for cognitive radio. *Progress In Electromagnetics Research*, 2016, 67: 11-20
[17] SHARMA, Sonia; TRIPATHI, Chandra Charu. A novel reconfigurable antenna with separate sensing mechanism for CR system. *Progress In Electromagnetics Research*, 2017, 72: 187-196.
[18] "CST: Computer Simulation Technology Based on FIT Method," 2014
[19] KOLEY, Santasri; MITRA, Debjani. A frequency-reconfigurable elliptical monopole antenna for cognitive radio networks. *Turkish Journal of Electrical Engineering & Computer Sciences*, 2017, 25.3: 2535-2546.

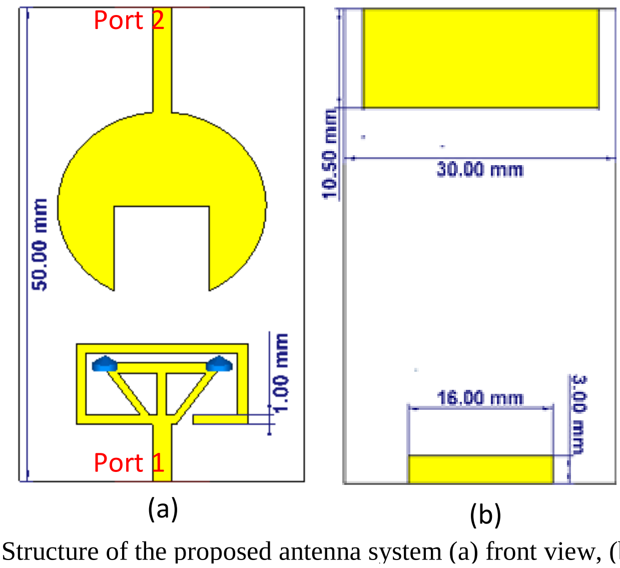

Figure 1: Structure of the proposed antenna system (a) front view, (b) back view

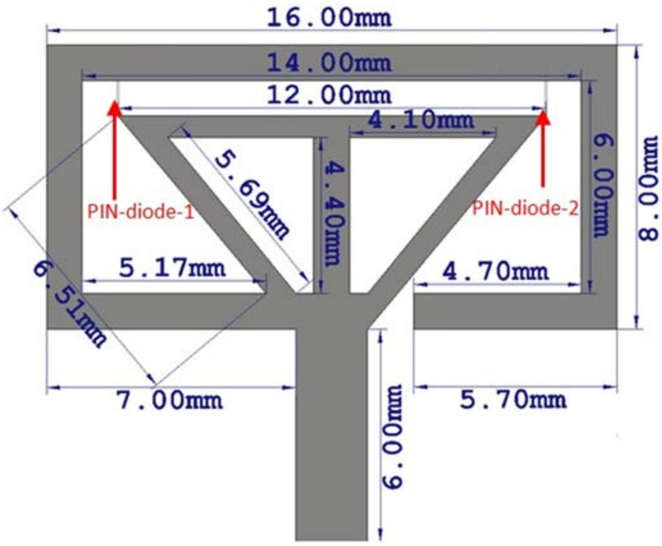

Figure 2: Structure of the reconfigurable communicating antenna.

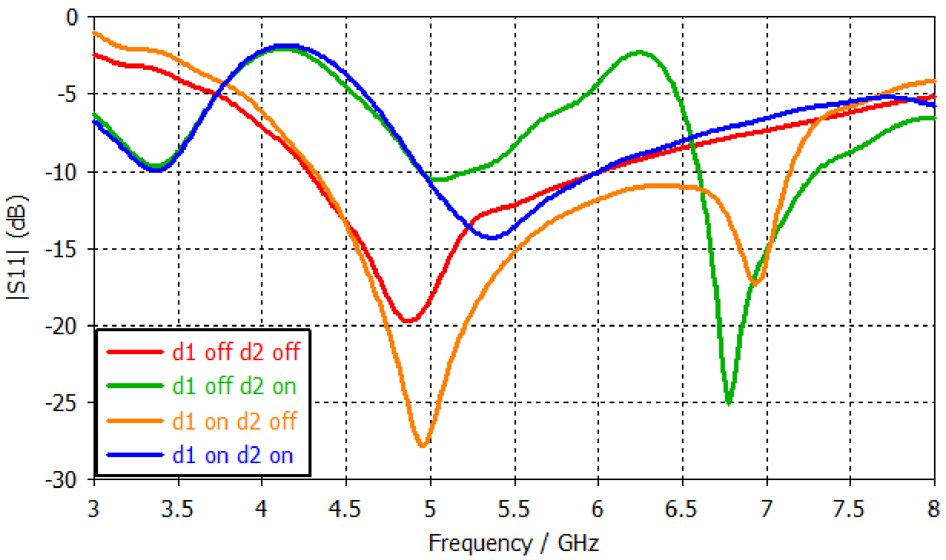

Figure 3: Simulated reflection coefficients for different PIN diodes states.

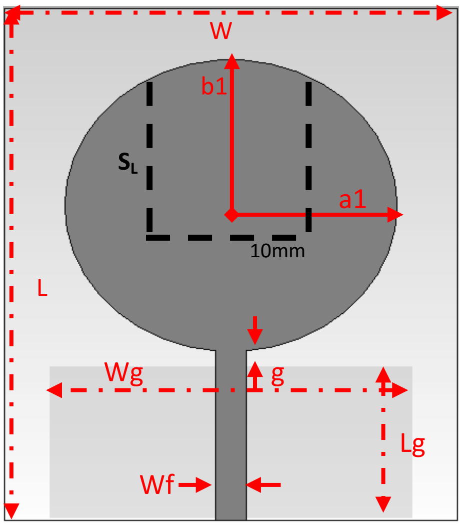

Figure 4: Structure of the elliptical monopole sensing antenna.

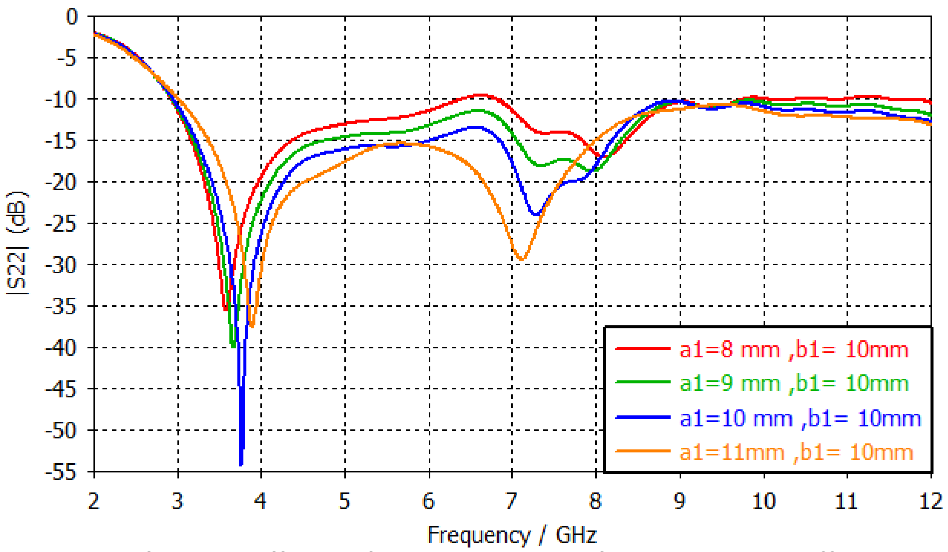

Figure 5: Reflection coefficient of the sensing antenna for w_g=24mm and different value axial ration.

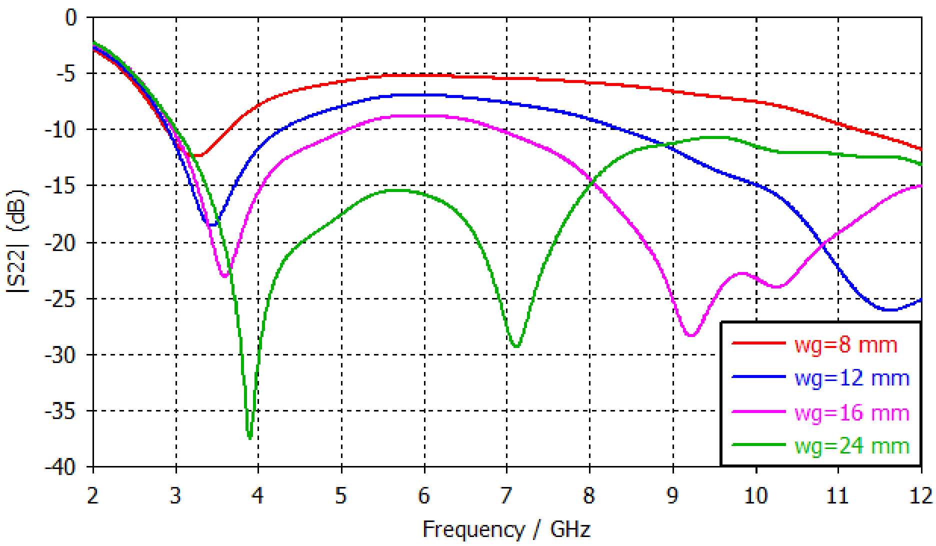

Figure 6: Reflection coefficient of the sensing antenna for a1=11mm, b1=10mm, and different value of ground plane width.

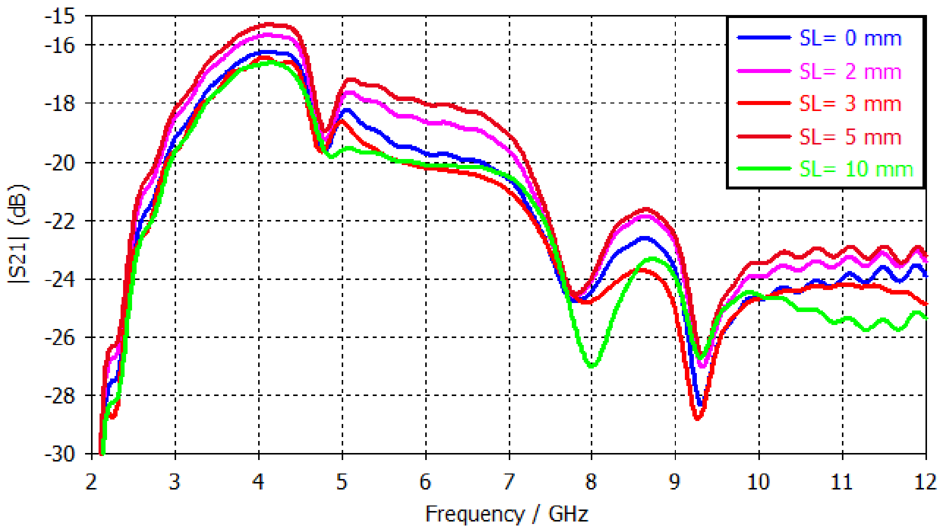

Figure 7: Mutual coupling of the proposed antenna system for different value of slot length.

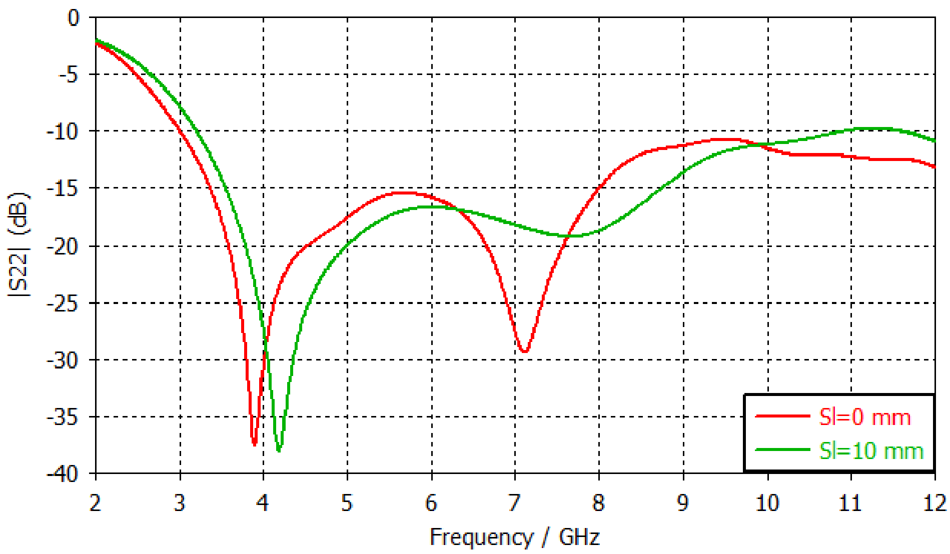

Figure 8: Comparison of the reflection coefficient of the sensing antenna with and without the slot.

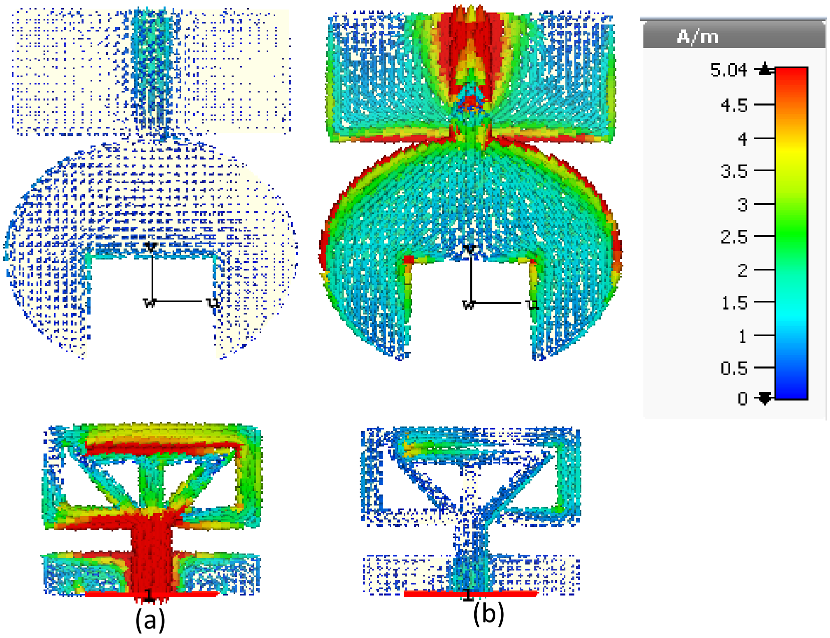

Figure 9: Current distribution of the propose antenna system at f=5GHz, and PIN diode -1 ON PIN diode-2 OFF when (a) port 1 is excited and (b) port 2 is excited.

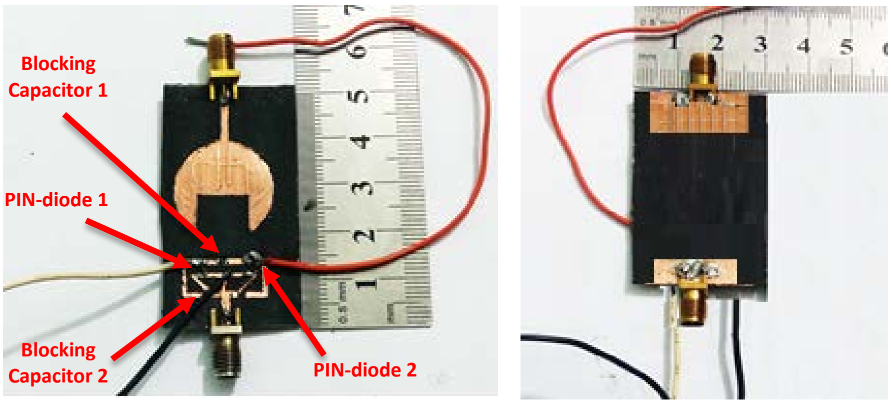

(a) (b)

Figure 10: Prototype of the proposed antenna system (a) front view (b) back view.

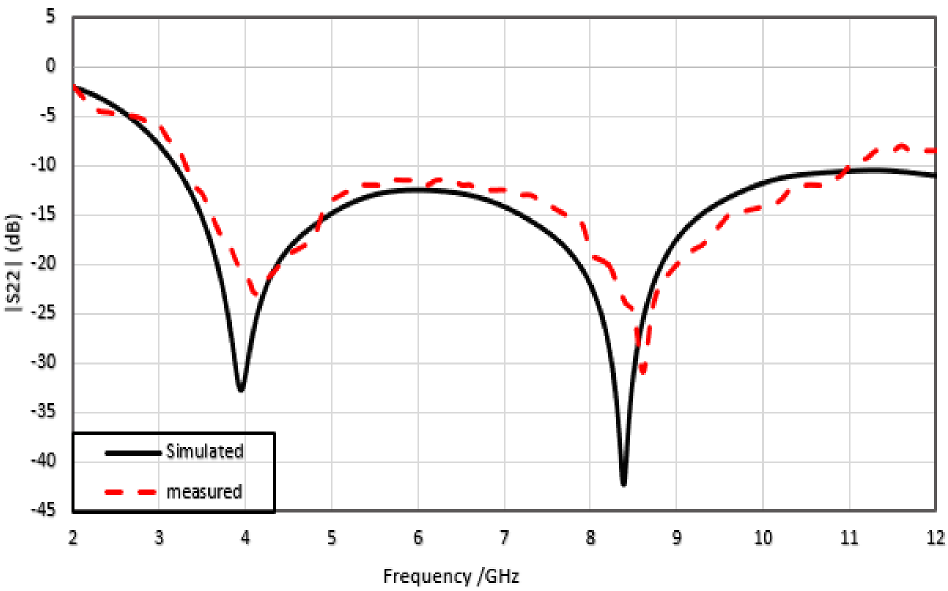

Figure 11: Simulated and measured reflection coefficient of the UWB sensing antenna.

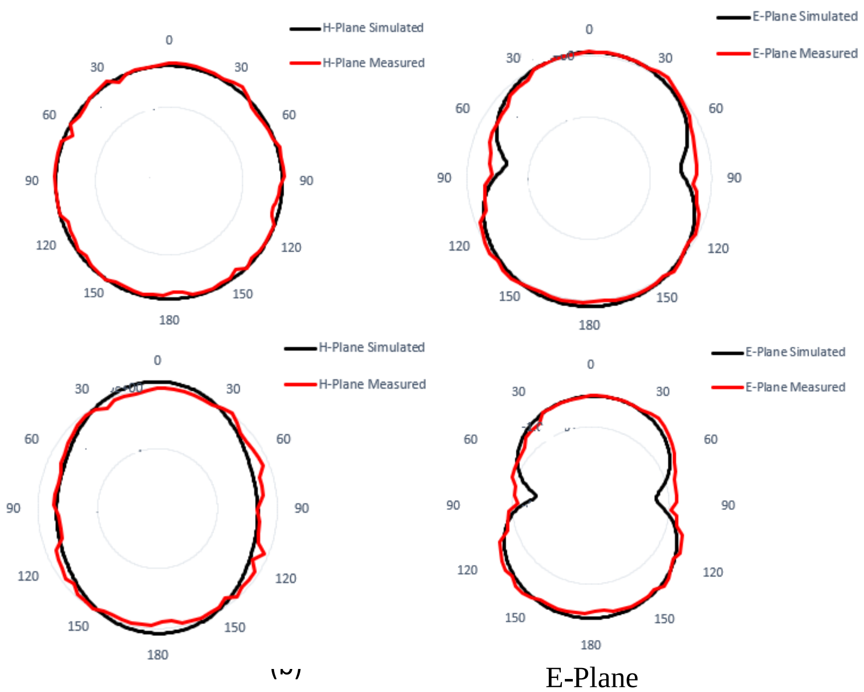

H-Plane E-Plane

Figure 12: Simulated and measured power patterns (a) E and H plane for 4GHz (b) E and H plane for 8.4GHz

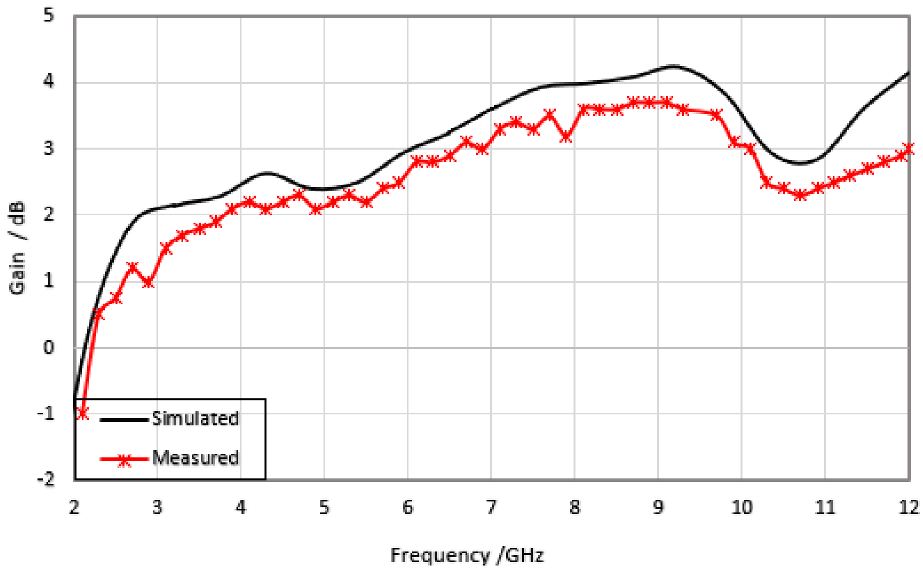

Figure 13: Simulated and measured gain for proposed sensing antenna.

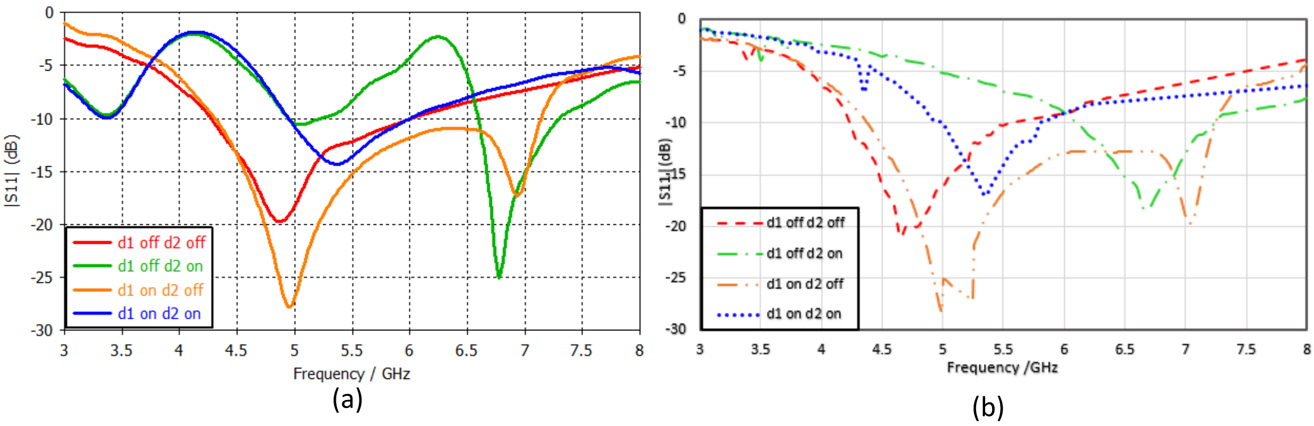

Figure 14: Reflection coefficients of the communicating antenna for different PIN diodes states (a) simulated and (b) measured.

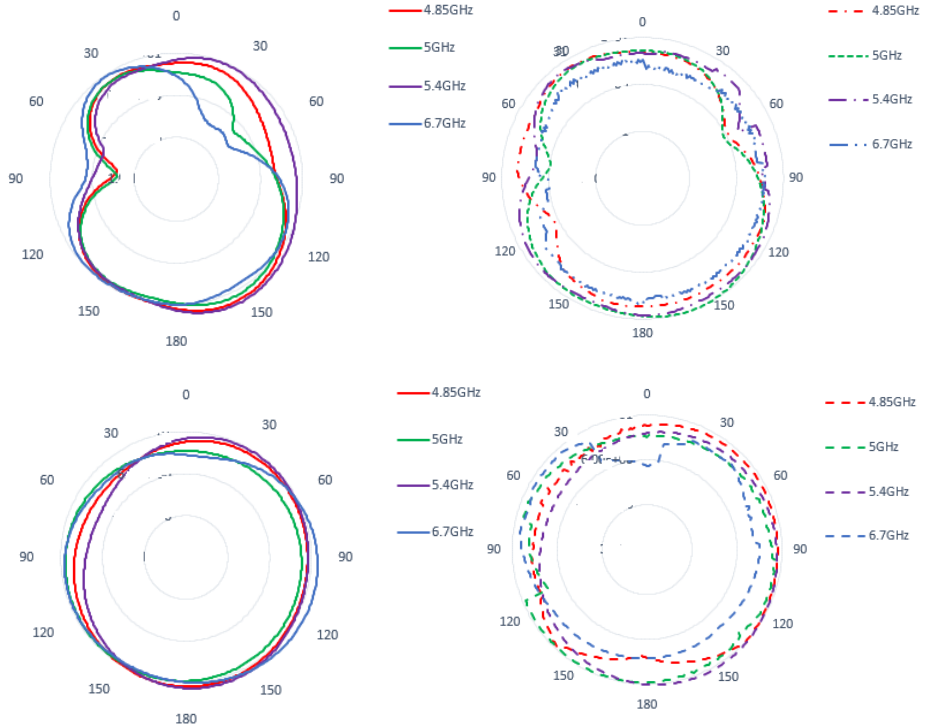

Simulated (b) Measured

Figure 15: Simulated and measured power patterns of the communicating antenna for different PIN diode states (a) E-PLANE (b) H-PLANE

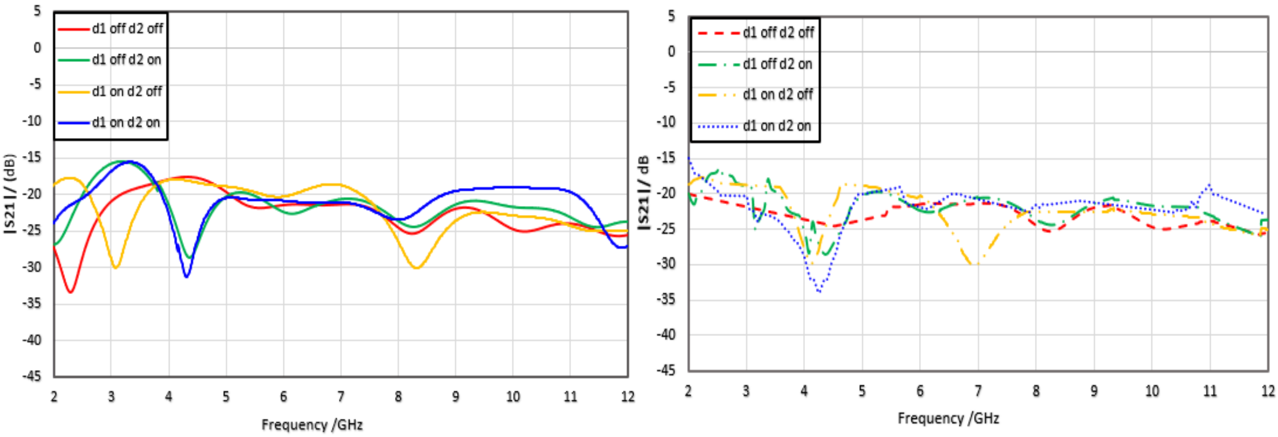

(a) (b)

Figure 16: Forward transmission coefficient of the proposed antenna system for different PIN diode states (a) simulated and (b) measured.